

Elastic electron scattering in quantum corrals: The importance of the shape of the adatom potential.

A. I. Rahachou^{1,*} and I. V. Zozoulenko^{1,†}

¹ *Department of Science and Technology (ITN),
Linköping University, S-601 74 Norrköping, Sweden*

(Dated: April 21, 2022)

We report elastic scattering theory for surface electron waves in quantum corrals defined by adatoms on the surface of noble metals. We develop a scattering-matrix technique that allows us to account for a realistic smooth potential profile of the scattering centers. Our calculations reproduce quantitatively all the experimental observations, which is in contrast to previous theories (treating the adatoms as point scatterers) that require additional inelastic channels of scattering into the bulk in order to achieve the agreement with the experiment. Our findings thus indicate that surface states are not coupled to the bulk electrons.

PACS numbers: 72.10.Fk, 73.20.At, 68.73.Ef, 03.65.Nk

Advances in modern nanotechnology made it possible to manipulate adatoms on the surface of a metal, arranging them into ordered structures coined as “quantum corrals”. Using the scanning tunneling microscopy (STM), Crommie *et al.*^{1,2,3} studied the scattering of the surface electron waves residing at (111) faces of Cu. These surface states interact strongly with Fe adatoms, and the spatial variation of the STM differential conductance revealed beautiful images of the standing wave patterns in the quantum corrals. In addition, the experiment showed a series of pronounced peaks in the energy spectrum of the differential conductance dI/dV at the center of the corrals.

In order to describe the experimental observation^{1,2}, Heller *et al.*⁴ have developed the multiple-scattering theory for surface electron waves in quantum corrals. In their theory each adatom was modelled as a point-like δ -function potential supporting isotropic s -wave scattering. The quantitative agreement with the experiment was achieved by assuming an additional (inelastic) channel of scattering (presumably into the bulk metallic states). The authors concluded that absorption is the dominant mechanism for the broadening of the energy levels seen in the experiment, and estimated that $\sim 25\%$ of the incident amplitude is reflected, $\sim 25\%$ is transmitted, and $\sim 50\%$ is absorbed. The importance of the electron scattering to the bulk states for the level width broadening in the quantum corrals was also asserted by Crampin *et al.*⁵ and Cramplin and Bryant⁶.

An alternative purely elastic scattering theory for the same quantum corral structures was reported by Harbury and Porod⁷. They modelled the adatoms by finite-height potential barriers, as opposed to “black dot” δ -point absorbing scattering potential adopted in the above cited works^{4,5,6}. The elastic theory accounts well for the spatial variation of the wave function in the quantum corrals, but overestimates the broadening of the resonant levels, especially for higher energies. The findings of Harbury and Porod therefore suggest that the features of the spectrum can be sensitive to the detailed shape of the scat-

tering potential.

It is important to stress that accounting for a detailed shape of a scattering potential was crucial for quantitative description of many phenomena in quantum nanostructures. This for example includes the Hall and bend resistance anomalies in four-terminal junctions⁸, the breakdown of quantized conductance in quantum point contacts calculated using realistic potentials⁹, the explanation of a branched flow in a two-dimensional electron gas¹⁰. In the present Brief report we develop a scattering matrix approach that allows us to account for a realistic smooth potential of the adatoms. We demonstrate that for such a potential the broadening and positions of the resonant states as well as the scattering wave function in the quantum corrals can be quantitatively described by the inelastic theory alone, without the assumption of any additional (inelastic) scattering channels. Our findings thus support the conclusions of Harbury and Porod⁷ that the adatoms do not significantly couple the surface-state electrons to the bulk metallic states.

The differential conductance dI/dV of the STM tunnel junction is proportional to the local density of states (LDOS) which is given in terms of the scattering eigenstates of the Hamiltonian \hat{H} , $\psi_q(\mathbf{r})$ ³,

$$dI/dV \sim \text{LDOS}(\mathbf{r}, E) = \sum_q |\psi_q(\mathbf{r})|^2 \delta(E - E_q). \quad (1)$$

In order to calculate the scattering eigenstates $\psi_q(\mathbf{r})$ we adopt to the problem at hand the scattering matrix technique¹¹ that was recently developed for numerical solution of the Helmholtz equation for resonant states of dielectric optical cavities with both complex geometry and variable refraction index. This is possible because of a direct correspondence between the Helmholtz and Schrödinger equations¹². The advantage of the scattering matrix technique is that it provides an efficient way to treat the smooth realistic profile of the adatom. Note that commonly used methods based on the discretization of the scattering domain would be rather impractical in terms of both computation power and memory, because

the smoothly varying potential of the adatom has to be mapped into a discrete grid with a very small lattice constant.

We consider a two-dimensional ring-shaped corral structure. Experimental observations suggest that adatoms strongly disturb the local charge density at the finite distance $\sim 7\text{\AA}^3$. An exact experimental shape of the adatom potential is not available. We thus model this potential as a Gaussian with the half-width σ and the height V_0 centered at the location (x_0, y_0) , $V(x, y) = V_0 \exp[-(x - x_0)^2/2\sigma^2] \exp[-(y - y_0)^2/2\sigma^2]$, (see below, inset to Fig. 3).

In order to calculate the scattering eigenstates we divide the quantum corral in inner, outer and intermediate regions. In the inner region (inside the corral) and in the outer region (outside the corral) the adatom potential is negligible, $V(x, y) = 0$. Therefore, in these two regions the solution to the Schrödinger equation can be written in analytical form. Introducing the polar coordinates we can write for the wave function outside the corral

$$\Psi^{out} = \sum_{q=-\infty}^{+\infty} \left(A_q H_q^{(2)}(kr) + B_q H_q^{(1)}(kr) \right) e^{iq\varphi}, \quad (2)$$

where $H_q^{(1)}, H_q^{(2)}$ are the Hankel functions of the first and second kind of the order q describing respectively incoming and outgoing waves; $k = \sqrt{2m^*E}/\hbar$, with m^* being the effective electron mass. The expression for the wave function inside the corral Ψ^{in} can be written in a similar fashion as an expansion over Bessel functions J_q .

We introduce the scattering matrix \mathbf{S} in a standard fashion^{11,12}, $B = \mathbf{S}A$, where A, B are column vectors composed of the expansion coefficients A_q, B_q for incoming and outgoing states in Eq. (2). The matrix element $\mathbf{S}_{q'q}$ gives the probability amplitude of scattering from an incoming state q into an outgoing state q' . In order to apply the scattering matrix technique we divide the intermediate region (i.e. the region where the adatom potential $V(x, y)$ is distinct from zero) into N narrow concentric rings. At each i -th boundary between the rings we introduce the scattering matrix \mathbf{S}^i that relates the states propagating (or decaying) towards the boundary, with those propagating (or decaying) away from the boundary. The matrices \mathbf{S}^i are derived using the requirement of continuity of the wave function and its first derivative at the boundary between the two neighboring rings. Successively combining the scattering matrixes for all the boundaries^{11,12}, $\mathbf{S}^1 \otimes \dots \otimes \mathbf{S}^N$, we can relate the combined matrix to the scattering matrix \mathbf{S} . With the help of the scattering matrix \mathbf{S} we determine the wave function in the outer region for every incoming state q in Eq. (2). Using the expression for the matrixes \mathbf{S}^i we then recover the corresponding wave functions in the intermediate region as well as the wave function Ψ^{in} in the inner region.

Note that in the scattering matrix technique one combines only two scattering matrixes at each step. Hence, it is not necessary to keep track of the solution for the

wave function in the whole space. This obviously eliminates the need for storing large matrices and facilitates the computational speed.

Using our scattering matrix technique we calculate the bias voltage dependence and the spatial distribution of the LDOS for 60-Fe-adatom, 88.7-Å-radius circular quantum corrals reported by Heller *et al.*⁴(Figs. 1 and 2). The Fe-adatoms are placed on the meshes of a 2.55Å triangular grid corresponding to the hexagonal Cu(111) lattice. The effective mass used in all the simulations was taken $m^* = 0.361m_0$ and the electron band-edge energy $E_0 = 0.43\text{eV}$ below the Fermi energy of the electrons^{1,7}. In the absence of applied voltage V these parameters correspond to the wavelength of electrons $\lambda = 30\text{\AA}$. For the parameters of the adatom potential we use⁷ $V_0 = 2.5\text{eV}$, $\sigma = 1.52\text{\AA}$ which correspond to those used by Harbury and Porod⁷ who modelled the adatoms as hard wall finite potential barriers of 1.52-Å diameter of the height of 2.5 eV.

Figure 1 also shows corresponding results of the multiple scattering theory of Heller *et al.*⁴. Both theories show a similar level of agreement with the experimental data in both the peak positions and level broadenings for the differential conductance as well as in the number and the peak positions for the spatial LDOS distribution throughout the cross-section of the quantum corral. But in contrast to the case of δ -scatterers used in Ref. [4] our model agrees quantitatively well with the experimental data without introduction additional inelastic scattering channels.

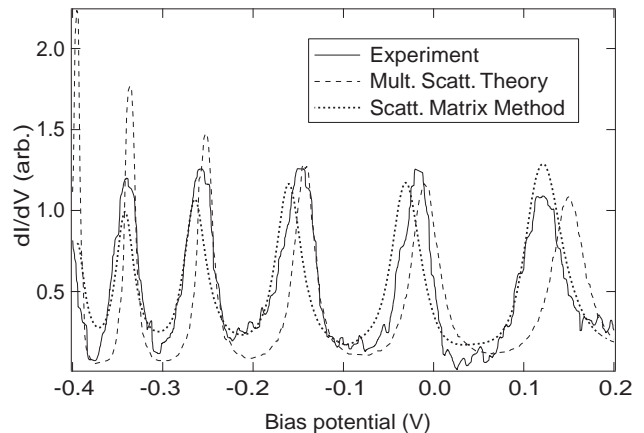


FIG. 1: The experimental spectrum of the differential conductance dI/dV at the center of the 88.7-Å-radius 60-Fe-adatom circular quantum corral structure on Cu(111) substrate (adopted from Ref. 4) (solid curve). The calculated spectrum, dotted line: Our scattering matrix technique applied for a smooth adatom potential with $V_0 = 2.5\text{eV}$, $\sigma = 1.52\text{\AA}$; dashed line: Multiple-scattering theory for δ -barrier adatom potential with inelastic channel of scattering (adopted from Ref. 4).

Figure 3 represents the differential conductance spectra dI/dV at the center of the quantum corral structure for various widths of adatom potentials σ . The in-

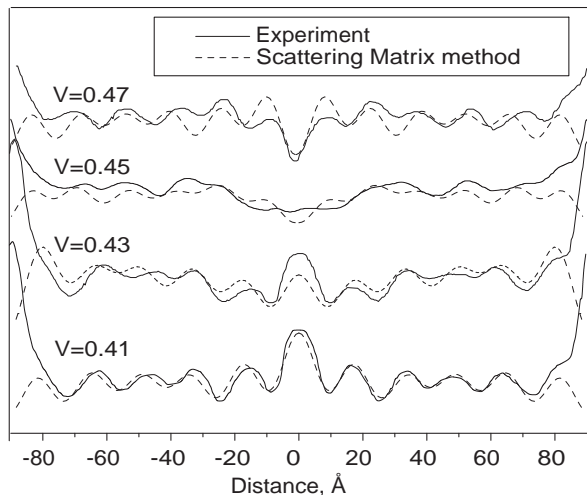


FIG. 2: The experimental curves (solid lines, adapted from Ref. 4) for the LDOS subject to the tip position inside a circular corral for low bias voltages. The calculated LDOS, dashed line: Our scattering matrix technique applied for a smooth adatom potential with $V_0 = 2.5eV$, $\sigma = 1.52\text{\AA}$; dot-dashed line: Multiple-scattering theory for δ -barrier adatom potential with inelastic channel of scattering (adopted from Ref. 4). Parameters of the structure and are the same as those in Figs. 1. Voltages are given in volts and measured relatively to the bottom of the surface-state band. All the theory voltages are shifted by -0.01 V relatively to the experiment.

crease in the potential width leads to significant narrowing of the peaks in the spectra due to stronger confinement of the wave function inside the corral. The best agreement with the experiment is achieved for $\sigma \approx 1.5\text{\AA}$, which is in agreement with the results reported by Harbury and Porod⁷. It is often assumed that because the spatial extent of the scattering potential ($\sigma \sim 7\text{\AA}$) is small compared to the wavelength of the incoming particles ($\lambda \sim 30\text{\AA}$), the adatom potential can be treated as a point scatterer or even as a continuous boundary $V(r) \sim \delta(r - r_0)$ ^{3,4,13}. The results presented in Fig. 3 clearly show that even though $\sigma \ll \lambda$, the finite width of the scattering potential affects strongly the observed characteristic of the systems. Our calculations thus signify the importance of the shape of the scattering potential for achieving the quantitative agreement with the experiment of the voltage dependence of dI/dV .

The experiment² suggests that for high energies of incoming electrons (i.e. for large tip voltages) the significant fraction of Fe ad atoms can move from their original positions. We therefore study the effect of this displacement on the shape and broadening of the resonant states of the quantum corral. Figure 4 shows the calculated differential conductance for a quantum corral for the case when the adatoms of an ideal circular corral are randomly shifted from their positions by one and two lattice constant (as illustrated in the insets to Fig. 4). One-lattice shift does not seem to have a significant effect on the

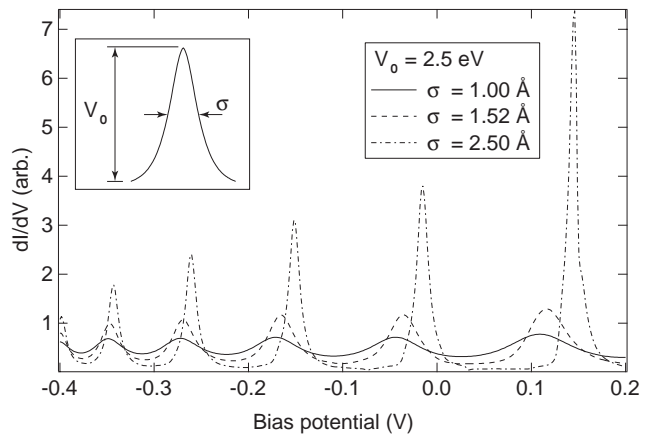


FIG. 3: The calculated spectrum of the differential conductance dI/dV at the center of the circular quantum corral structure for various widths σ of adatom potential for fixed barrier height $V_0 = 2.5eV$. Parameters of the structure are the same as those in Fig. 1. Inset shows the schematic shape of the potential.

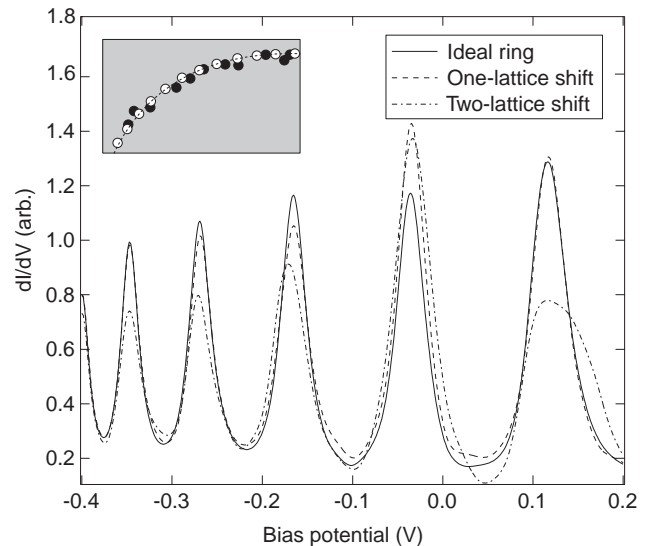


FIG. 4: Effect of the non-ideal positioning of the adatoms on the differential conductance of the quantum corral. Parameters of the structure and the adatom potential are the same as those in Figs. 1 and 2. Inset illustrates the displacement of the scatterers from their ideal positions (white circles) in a circular geometry for two-lattice shift.

broadening of the peaks in the differential conductance. The deviation from an ideal circular case become rather noticeable for the shift in adatom positions by two lattice sites. As expected, these deviations are more pronounced for larger energies of incoming electrons. Note that we performed simulations for different realization of the ensembles of scatterers (keeping the average shift fixed to one or two lattice sites), and all of them are almost indistinguishable. This is because of the self-averaging character of scattering in a quantum corral due to a large

number of scatterers. Our calculations thus pinpoint the deviation from a regular arrangements of scatterers as an additional factor that should be taken into account for achieving the quantitative agreement with the experiment.

To conclude, we studied the scattering of electron waves by quantum corral structure for the case of realistic smooth potential of adatom scatterers. We achieved a detailed agreement with the experiment without introducing the additional inelastic channels of scattering.

Our results thus support the theory that adatoms do not significantly couple the surface-state electrons to the bulk states. Our findings also suggest that accounting for a realistic potential shape may be of particular importance for the quantitative description of quantum mirages experiments.

Financial support from Vetenskapsrådet (I.V.Z) and the National Graduate School of Scientific Computing (A. I. R.) is gratefully acknowledged. We appreciate a discussion with G. Hansson.

* Electronic address: alira@itn.liu.se

† Electronic address: igozo@itn.liu.se

¹ M. F. Crommie, C. P. Lutz, and D. M. Eigler, *Nature* **363**, 524 (1993).

² M. F. Crommie, C. P. Lutz, and D. M. Eigler, *Science* **262**, 218 (1993).

³ for the review see, G. A. Fiete and E. J. Heller, *Rev. Mod. Phys.* **75**, 933 (2003).

⁴ E. J. Heller, M. F. Crommie, C. P. Lutz, and D. M. Eigler, *Nature* **369**, 464 (1994).

⁵ S. Crampin, M. H. Boon, and J. E. Inglesfield, *Phys. Rev. Lett.* **73**, 1051 (1994).

⁶ S. Crampin and O. R. Bryant, *Phys. Rev. B* **54** R17367 (1996).

⁷ H. K. Harbury and W. Porod, *Phys. Rev. B* **53** 15455 (1996).

⁸ H. U. Baranger, D. P. DiVincenzo, R. A. Jalabert, and A. D. Stone, *Phys. Rev. B* **44**, 10 637 (1991).

⁹ Laughton, J. A. Nixon, J. H. Davies, and H. U. Baranger, *Phys. Rev. B* **43**, 12638 (1991); M. Laughton, J. R. Barker, J. A. Nixon, and J. H. Davies; *ibid.*, **44** 1150 (1991).

¹⁰ M. A. Topinka, B. J. LeRoy, R. M. Westervelt, S. E. J. Shaw, T. Fleischmann, E. J. Heller, K. D. Maranowski, and A. C. Gossard, *Nature*, **410**, 183 (2001).

¹¹ A. I. Rahachou and I. V. Zozoulenko, *J. Appl. Phys.* **94**, 7929 (2003); A. I. Rahachou and I. V. Zozoulenko, *Applied Optics*, **43**, in press (March 2004) (arXiv:physics/0307024).

¹² S. Datta, *Electronic Transport in Mesoscopic Systems* (Cambridge University Press, Cambridge, 1995)

¹³ A. Lobos and A. A. Aligia, *Phys. Rev. B* **68**, 035411 (2003).